ACCOUNTS
of chemical research

Solid-State NMR in Macromolecular Systems: Insights on How Molecular Entities Move

MICHAEL RYAN HANSEN,* ROBERT GRAF,* AND
HANS WOLFGANG SPIESS*

Max Planck Institute for Polymer Research, Ackermannweg 10, D-55128 Mainz, Germany

RECEIVED ON DECEMBER 18, 2012

CONSPECTUS

The function of synthetic and natural macromolecular systems critically depends on the packing and dynamics of the individual components of a given system. Not only can solid-state NMR provide structural information with atomic resolution, but it can also provide a way to characterize the amplitude and time scales of motions over broad ranges of length and time. These movements include molecular dynamics, rotational and translational motions of the building blocks, and also the motion of the functional species themselves, such as protons or ions. This Account examines solid-state NMR methods for correlating dynamics and function in a variety of chemical systems.

In the early days, scientists thought that the rotational motions reflected the geometry of the moving entities. They described these phenomena as jumps about well-defined axes, such as phenyl flips, even in amorphous polymers. Later, they realized that conformational transitions in macromolecules happen in a much more complex way. Because the individual entities do not rotate around well-defined axes, they require much less space. Only recently researchers have appreciated the relative importance of large angle fluctuations of polymers over rotational jumps. Researchers have long considered that cooperative motions might be at work, yet only recently they have clearly detected these motions by NMR in macromolecular and supramolecular systems.

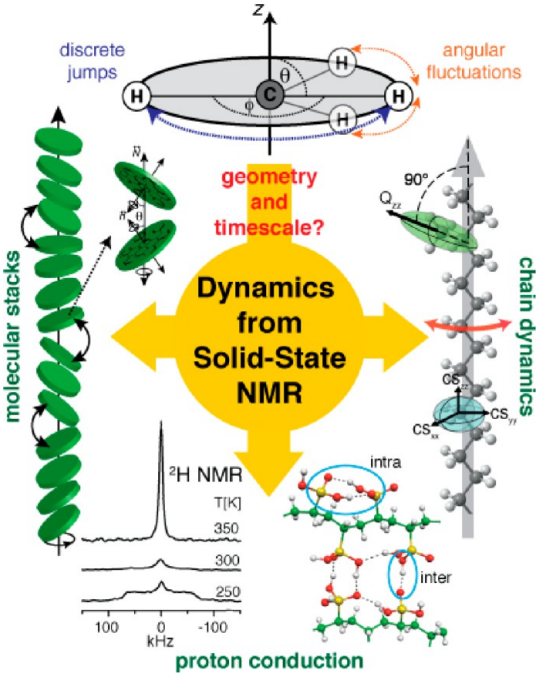

In correlations of dynamics and function, local motions do not always provide the mechanism of long-range transport. This idea holds true in ion conduction but also applies to chain transport in polymer melts and semicrystalline polymers. Similar chain motions and ion transport likewise occur in functional biopolymers, systems where solid-state NMR studies are also performed. In polymer science, researchers have appreciated the unique information on molecular dynamics available from advanced solid-state NMR at times, where their colleagues in the biomacromolecular sciences have emphasized structure. By contrast, following X-ray crystallographers, researchers studying proteins using solution NMR introduced the combination of NMR with computer simulation before that became common practice in solid-state NMR. Today's simulation methods can handle partially ordered or even disordered systems common in synthetic polymers. Thus, the multitechnique approaches employed in NMR of synthetic and biological macromolecules have converged. Therefore, this Account will be relevant to both researchers studying synthetic macromolecular and supramolecular systems and those studying biological complexes.

Introduction

With emphasis on elucidating molecular dynamics, we first briefly review how NMR interactions can probe geometry and time scale of molecular motions via *isotropic* and *anisotropic* nuclear spin interactions. These include the isotropic and anisotropic chemical shifts, homo- and heteronuclear

Published on the Web 03/13/2013 www.pubs.acs.org/accounts
10.1021/ar300338b

TABLE 1. NMR Interactions Used for Characterizing Dynamics in Polymers and Macromolecular Systems.[a]

	chemical shift (anisotropy)	dipole-dipole coupling	quadrupole coupling
typical magnitude	0−200 ppm	2−30 kHz (at typical bond distance)	100−150 kHz (for ^{2}H)
electronic structure	yes	no	yes
geometry	intrinsic and orientation	internuclear distance and orientation	intrinsic and orientation
typical nuclei	^{1}H, ^{13}C, ^{15}N, ^{19}F, ^{29}Si, ^{31}P	^{1}H, ^{13}C, ^{15}N, ^{19}F, ^{29}Si, ^{31}P	^{2}H, ^{14}N, ^{17}O
dynamics	conformational transitions, rotational motions	translational and rotational motions	rotational motions

[a]The typical magnitudes of the interactions depend on the type of nucleus.

dipole−dipole couplings, and quadrupole couplings.[1] A more detailed description of these interactions and the NMR techniques available for probing them are available in several reviews.[2−4] This is followed by considering typical jump angles for organic molecules, angular fluctuations of different mean amplitudes, and available software for calculating averaged tensors. Last, but not least, experimental examples are reviewed, mostly taken from our own work.

Solid-State NMR and Molecular Dynamics

Anisotropic Nuclear Spin Interactions. The wealth of information accessible by solid-state NMR spectroscopy results from the sensitivity of the anisotropic nuclear spin interactions toward their immediate surroundings, see Table 1. The chemical shift provides the basis of site selectivity, where geometric parameters such as internuclear vectors can be encoded via dipole−dipole couplings. Of the molecular motions in polymers, rotations have the most pronounced effects, because the spin interactions are angular dependent. However, conformational dynamics and translational motions can be tackled as well.

For couplings with magnitudes much weaker than the Zeeman interaction, first-order perturbation theory can be applied, and the resulting orientation-dependent NMR frequency takes the form[1]

$$\omega(\Theta_\lambda, \Phi_\lambda) - \omega_L = \omega_{iso} + \frac{\Delta_\lambda}{2}(3\cos^2\Theta_\lambda - 1 - \eta_\lambda \sin^2\Theta_\lambda \cos 2\Theta_\lambda) \quad (1)$$

Here, ω_L is the Larmor frequency and ω_{iso} is the isotropic frequency component, while the remaining terms describe angular-dependent contributions. The magnitude of the anisotropy is specified by Δ_λ with η_λ as the asymmetry parameter, describing the deviation from *axial* symmetry. The subscript λ denotes the three nuclear spin interactions, namely, chemical shift anisotropy (CSA), dipole−dipole coupling (DDC), and quadrupole coupling (QC). For each of these interactions, a coordinate frame of reference (the so-called principal-axes system, PAS) is defined, in which the interaction tensor is diagonal. The orientation of the PAS with respect to the external magnetic field is denoted by the polar angles Θ_λ and Φ_λ. These angles can differ or be alike for different interactions. In organic solids, the PASs are often directly linked to the molecular geometry, for example, for aromatic rings the unique axis (λ_{zz}) of the ^{13}C CSA is perpendicular to phenyl plane, while the heteronuclear ^{13}C−^{1}H DDC and ^{2}H QC are directed along the C−H bond directions.[1]

In solid samples, a so-called powder average, with equal probability for all directions, yields a broad, yet characteristic NMR spectrum that reflects the magnitude of *anisotropic spin interaction*.[1] Typical examples are shown in Figure 1 for the static case and under magic angle sample spinning (MAS), where the spectrum is split into sidebands at multiples of the spinning frequency, ω_R. Such sideband patterns offer high spectral resolution, while keeping the information about the anisotropic interaction. For infinitely high ω_R, only the isotropic frequency component (ω_{iso}) is retained due to averaging of the angular-dependent terms, as in solution.

Motional Averaging. If the residue studied undergoes an anisotropic motion with a rate Ω exceeding the anisotropy Δ_λ, an averaged coupling tensor results,[1] and the orientation-dependent NMR frequency can again be described by an equation similar to eq 1,

$$\omega_\lambda(\vartheta_\lambda, \varphi_\lambda) - \omega_L = \omega_{iso} + \frac{\delta_\lambda}{2}(3\cos^2\vartheta_\lambda - 1 - \bar{\eta}_\lambda \sin^2\vartheta_\lambda \cos 2\varphi_\lambda) \quad (2)$$

yet with reduced magnitude δ_λ and different asymmetry parameter $\bar{\eta}_\lambda$, see Figure 1c,d. Moreover, the averaged coupling tensors will have different PASs, whose orientation with respect to the external magnetic field is described by polar angles, ϑ_λ and φ_λ. It should be noted that $\bar{\eta}_\lambda$ can be unequal to zero even if $\eta_\lambda = 0$. A fast axial motion of a second-rank tensor about a fixed axis involving three or more equivalent sites, however, will lead to an axially symmetric averaged tensor with $\bar{\eta}_\lambda = 0$. A prominent example often met in stacks of aromatic moieties is the axial rotation around the column axis. Here, λ_{zz} for all

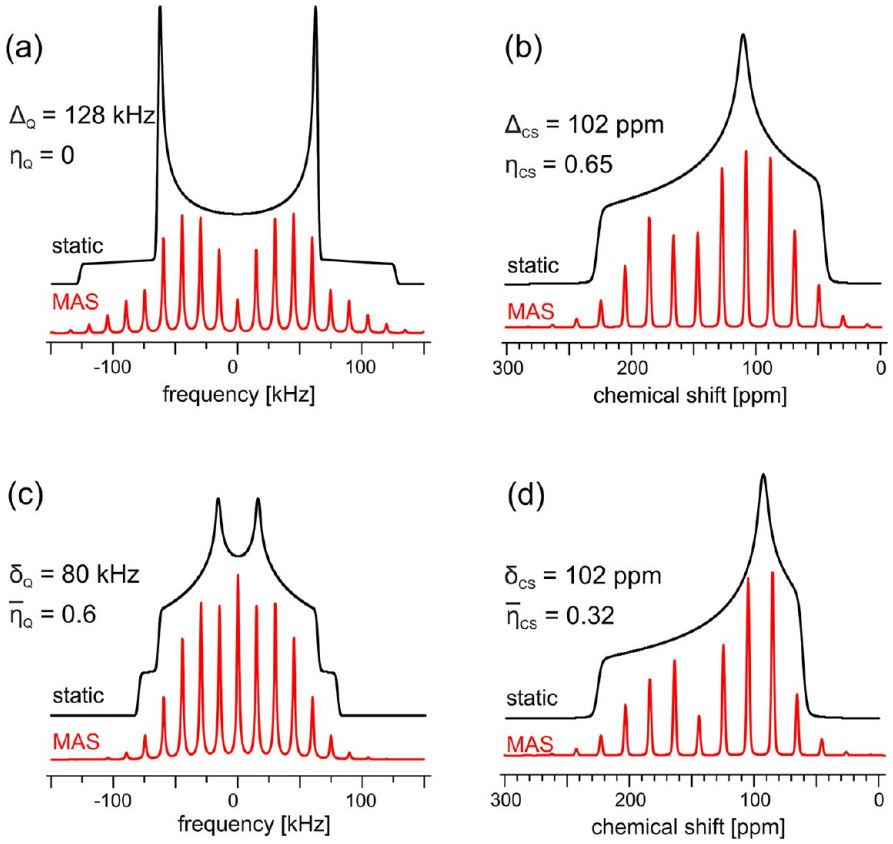

FIGURE 1. Simulated (a, c) ^{2}H and (b, d) ^{13}C NMR spectra of (a, b) rigid and (c, d) flipping phenylene rings under static and MAS conditions ($\omega_{MAS,^2H} = 15$ kHz, $\omega_{MAS,^{13}C} = 20$ ppm).

anisotropic interactions is parallel to the column axis, reducing the coupling for ^{2}H QC and ^{13}C–^{1}H DDC by a factor of 2, but only slightly for ^{13}C CSA. Such an average tensor will result for each site irrespective of how complicated the rotational motion may be as long as it is uniform.

Dynamic Order Parameters. Often, only the reduced coupling magnitude, δ_λ, is accessible through a specific experiment, particularly under MAS, see below. Then it is still useful to consider the ratio between δ_λ and Δ_λ. This ratio is the well-known *order parameter* S in liquid crystals (LC), where the mesogens perform axial motions around the director.[5] Thus, considering a *dynamic order parameter*

$$S_\lambda = \frac{\delta_\lambda}{\Delta_\lambda}, \quad \text{with} \quad 0 \le S_\lambda \le 1 \tag{3}$$

turns out to be extremely useful in order to specify the amplitude of rotational motions. Since S_λ is an intrinsic quantity of the system under study, it implies neither local ordering nor a macroscopically ordered system. However, because PAS$_\lambda$ can have different orientations with respect to the molecular entities, S_λ can be different for different interactions. Simultaneous determination of S_λ for different spin interactions is particularly informative, because the characteristics of the motional process will affect the anisotropic spin interactions in different ways.

Distribution of Correlation Times. For a complete characterization of molecular motions, knowledge about the amplitudes of the motion is not sufficient; one has to also know the *correlation time*, τ_c, of the motion. In addition to NMR, τ_c can be obtained from dielectric spectroscopy[6] or light scattering.[7] The most pronounced changes in the solid-state NMR line shapes occur, when the correlation rate, $\Omega = 1/\tau_c$, is comparable to Δ_λ or δ_λ, ω_R, or the magnitude of the applied radio frequency field.[1,4] This situation is typically referred to as the *intermediate exchange* region, where interference effects cause severe losses of intensity often quantified by a reduction factor. However, in polymers, processes with a single correlation time are rarely found.[8] Instead, the correlation times for a specific process can easily span several orders of magnitude, attributed to slight variations of the activation enthalpy for local rotations in a thermally activated process.[1] As an illustrative example, Figure 2 considers a Gaussian distribution of τ_c on a logarithmic scale covering about three orders of magnitude.[9] For

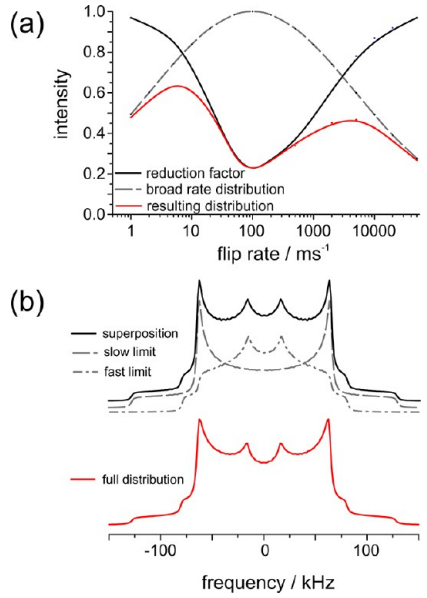

FIGURE 2. (a) Reduction factor of the intermediate motional regime characteristic of a phenylene flip motion with a broad correlation time distribution and its resulting distribution function. (b) Simulated ^{2}H solid-echo NMR spectra for a phenylene group (isotropic powder) in the slow and fast motional limits, their superposition, and full simulation. Spectral parameters as in Figure 1a,c.

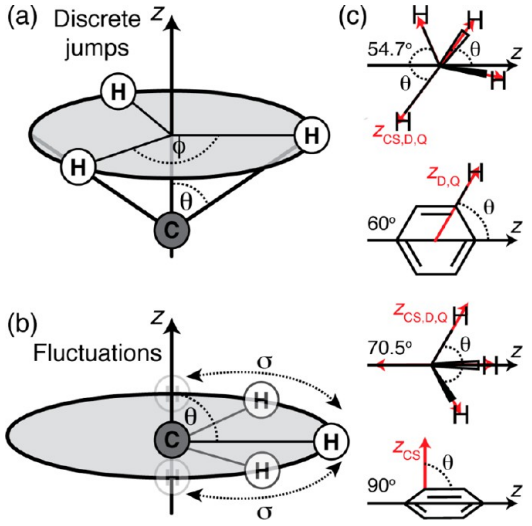

FIGURE 3. Cone models illustrating the definitions of θ, φ, and σ for (a) discrete jumps and (b) angular fluctuations. (c) Characteristic θ angles for a number of organic building blocks. Black arrows indicate the main axis of the cone model (z), and red arrows indicate the direction of the unique tensor element (λ_{zz}) of the given NMR interactions ($z_{CS,D,Q}$).

modeling the ^{2}H NMR line shape, the distribution of τ_c has to be convoluted with the reduction factor for each τ_c, see Figure 2a. The resulting ^{2}H solid-echo NMR line shapes for a simple case like the phenyl flip (Figure 1) are plotted in Figure 2b. Remarkably, a simple weighted superposition of the ^{2}H spectra in the slow and the fast motional regimes, neglecting the spectra of the intermediate regime, already provides an excellent description for such a broad distribution of correlation times (Figure 2b).

Rotational Jumps and Angular Fluctuations. Molecules or segments of larger chemical structures often undergo different kinds of motions as a function of temperature, inducing phase transitions, or even facilitating a molecular function. As discussed above for phenylene flips (Figure 1), this leads to a reduction of the rigid ^{2}H QC that depends on its specific tensor and motion geometries. Several simulation packages have been developed to deal with such discrete jumps,[10,11] where our group has contributed with the NMR WEBLAB.[12] This browser-based software utilizes the cone model (Figure 3a), and Figure 3c depicts characteristic θ angles and NMR tensor orientations for λ_{zz}.

NMR interactions can also be averaged by fast-limit *angular fluctuations* as sketched in Figure 3b, an important aspect, not often discussed in the literature. To acknowledge this point, the NMR WEBLAB now includes treatment of angular fluctuations (Gaussian or box distributions) for discrete jumps between multiple sites and single NMR interactions.[13] Here we focus on single NMR interactions, summarizing the results for axial and nonaxial NMR tensors, in Figures 4 and 5, respectively. The axial case is particularly important to determine site-specific dynamic order parameters (eq 3) for X$-^1$H DCCs and ^{2}H QCs, since the static anisotropy (Δ_λ) is well-known. Figure 4a,b shows the dependence of the reduced anisotropy (S_λ) and asymmetry (η_λ) on the cone angle (θ) and Gaussian fluctuation angle (σ), see Figure 3b. S_λ is easily reduced by a factor of 2 for moderate θ and σ, comparable to the situation of 180° flips, and even down to zero, when θ approaches the magic angle 54.7° (Figure 4c). In contrast, η_λ is much less sensitive but fluctuates significantly for large θ angles (Figure 4d). It should be mentioned that η_D is often hard to determine precisely from solid-state NMR experiments,[14] while the magnitude (D) is fully accessible.[15] Thus, on the basis of the plots shown in Figure 4, it is possible to determine how much a molecular group or segment is fluctuating from experimentally determined X$-^1$H DCCs and ^{2}H QCs. Such information is highly valuable when relating averaged anisotropic NMR parameters to a specific motion or molecular function.[16]

For nonaxial tensors, the λ_{xx} and λ_{yy} tensor elements have different magnitudes, and angular fluctuations will lead to a mixed averaging of these components. Therefore, the NMR tensor orientation has to be known and specified by

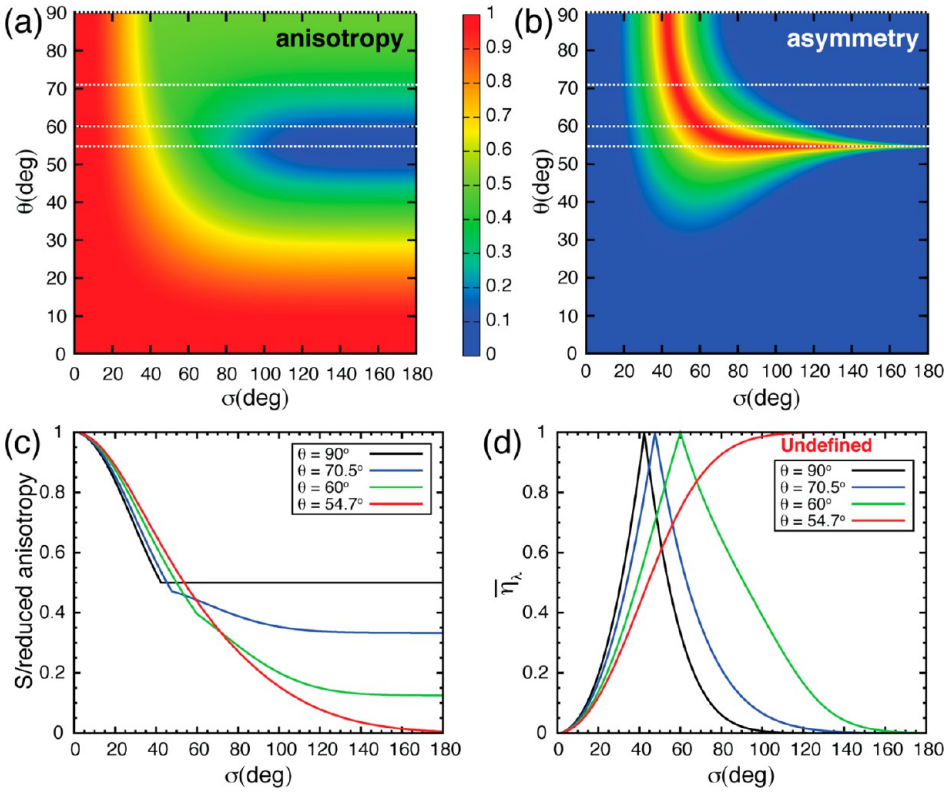

FIGURE 4. Fast-limit single-site angular fluctuations of a CS, D, or Q tensor with axial symmetry (rigid limit) described by a Gaussian distribution (see Figure 3b). (a,b) Normalized reduction of the tensor anisotropy, S_λ, and value of the asymmetry parameter (η_λ) according to the color scale bar. (c,d) Traces for characteristic θ angles. Note that η_λ is undefined for large angle fluctuations with $\theta = 54.7°$, causing δ_λ to vanish (proportional to λ_{zz}).

the polar tensor angle (α), see Figure 5a. Such a situation often arises when dealing with ^{13}C CSAs and ^{2}H QCs. Figure 5b,c summarizes the results for such cases with different η_λ and α.

NMR as Part of a Multitechnique Approach

Advances in synthesizing, characterizing, and understanding macromolecular and supramolecular systems have led to an enormous variety and complexity in the field of polymer science. As outlined in a recent *Perspective Article*,[17] the traditional separation in terms of structure vs dynamics, crystalline vs amorphous, or experiment vs theory is increasingly overcome. In fact, no experimental or theoretical/simulation approach alone can provide the full information. Instead, multitechnique approaches are needed, and conclusions should be supported by as many complementary techniques as possible (Figure 6). Combining X-ray diffraction (XRD) or NMR spectroscopy with computer simulations is well established nowadays for studies of structure and dynamics in biomacromolecules[18] and microcrystalline systems.[19] Recently, a systematic strategy for revealing the local packing in semicrystalline polymers was described,[20] where unit-cell parameters are derived from XRD and combined with molecular constraints from solid-state NMR. These experimental results are unified by quantum-chemical calculations, considering specific packing models *in silico* thereby quantifying π-stacking effects. In addition, the amount of disordered, amorphous regions is quantified.[20]

Elucidating slow dynamics in combination with simulations are currently limited by the current capability of computers. The much faster motions accessible by neutron scattering or NMR relaxation, however, can already be analyzed by computer simulation.[25] Advantage should be taken of the fact that a general formalism exists, which does not involve the usual assumption of exponential relaxation[26] as demonstrated recently for ^{2}H and ^{17}O relaxation in water.[27] Remarkably, the simulated correlation functions differ significantly from simple exponentials. For dynamics in macromolecules, the combination of NMR and dielectrics is particularly informative.[28] The latter can nowadays routinely cover many orders of magnitude for τ_c, whereas NMR due its site-selectivity can identify the moving groups.

Elucidating the geometry of motion for ions is particularly important for unraveling proton conduction mechanisms or ion conductivity.[30,31] In poly(vinyl phosphonic acid), ^{1}H, ^{2}H,

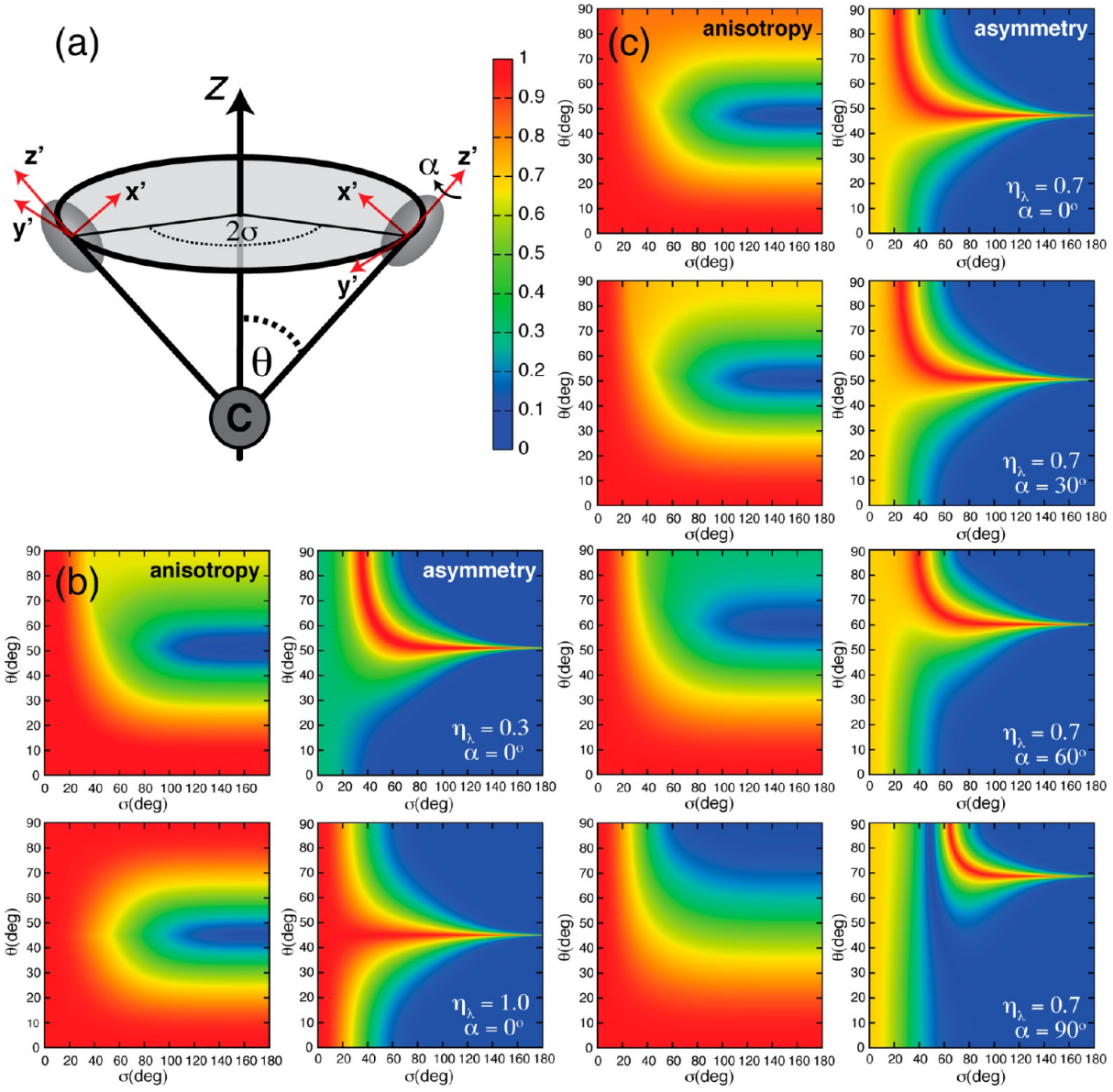

FIGURE 5. (a) Single-site angular fluctuation for a CSA or Q tensor with nonaxial symmetry illustrating the definitions of θ, σ, and polar tensor angle α. (b, c) The rigid limit values for η_λ and α are given on each 2D contour plot with the color-scale bar showing the normalized fast-limit value of S_λ and η_λ.

^{13}C, and ^{31}P NMR combined with computer simulations provided a detailed picture of a highly *disordered* hydrogen-bonded network, Figure 7, allowing for a remarkable proton conductivity.[29,32]

In both synthetic macromolecules and biomacromolecules, course-grained information about the structure on intermediate length scales and dynamics in the nanosecond range is of interest. Here, EPR spectroscopy experiences a remarkable revival.[33] Distance measurements on the nanometer scale by double electron−electron resonance (DEER) have become a prominent tool for elucidating the structure of disordered proteins or refolding of the integral membrane protein complexes.[34]

Applications to Macromolecular Systems

Twist Motions in Crystalline Polymers. The easiest case of chain motion occurs in the crystalline regions of semicrystalline polymers like high-density polyethylene (PE). In addition to the long-range chain motion,[35] motions of defects, for example, branches in the crystal itself, are of particular interest. Combining state-of-the-art synthetic chemistry, providing samples with well-defined branch identity and spacing, and solid-state NMR spectroscopy, one can then address the following questions:[36] What is the nature of the motion of the branches? How do the branches alter the geometry and mobility of adjacent chain segments? Does the motion of one branch influence the motion of

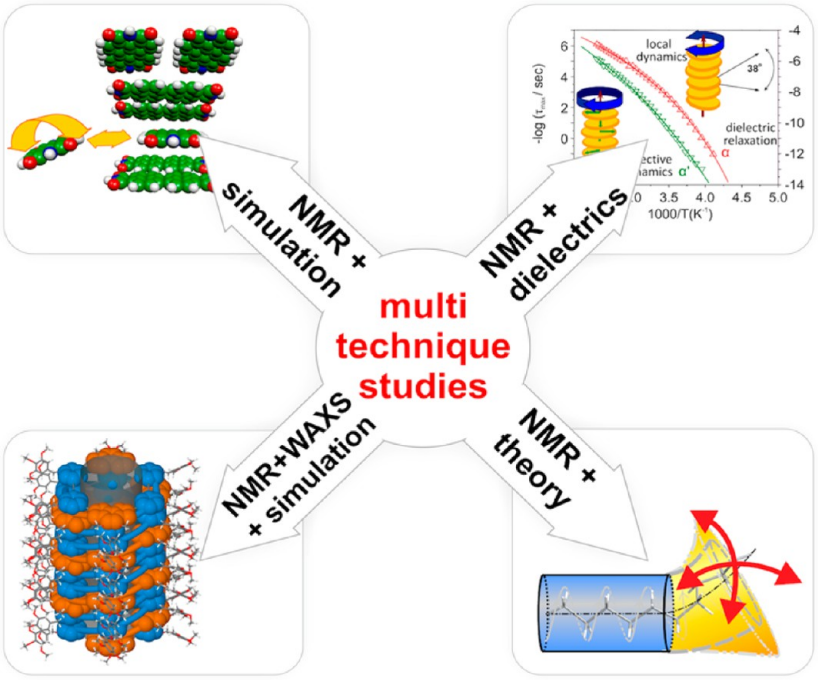

FIGURE 6. Schematic representation of the multitechnique approach needed to study structure and dynamics of macromolecules.[21−24]

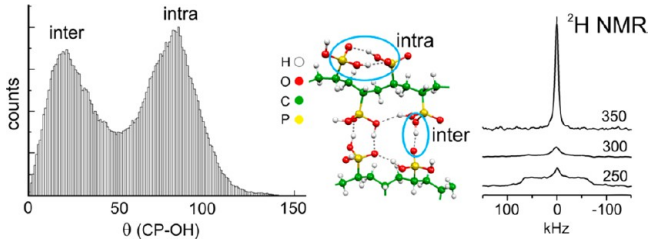

FIGURE 7. (left) Distribution of the CP−OH angle within a given phosphonic acid group of poly(vinyl phosphonic acid), PVPA, predicted from first-principles molecular dynamics simulations. (right) Experimental ^{2}H NMR line shapes as a function of temperature. Reproduced from ref 29. Copyright 2007 American Chemical Society.

neighboring branches (collective motion, rotator phase)? In Figure 8b simulated NMR line shapes for both ^{2}H and ^{13}C NMR are plotted. Because the unique axes of both NMR interactions are perpendicular to each other (Figure 8a), different scenarios can easily be distinguished. Samples with methyl branches separated by more than 20 methylene groups exhibit fluctuations of about ±40° around the chain axis. The segmental motion of the polymer chains between the branching sites can be monitored via the ^{13}C CSA. This reveals a twist motion centered at the branching sites. For shorter spacing, for example, 14 CH_2 units between subsequent methyl branches, collective twists occur, ultimately leading to a rotator phase. Thus, localized and collective mobility induced by the defects can clearly be distinguished, Figure 8c,d.

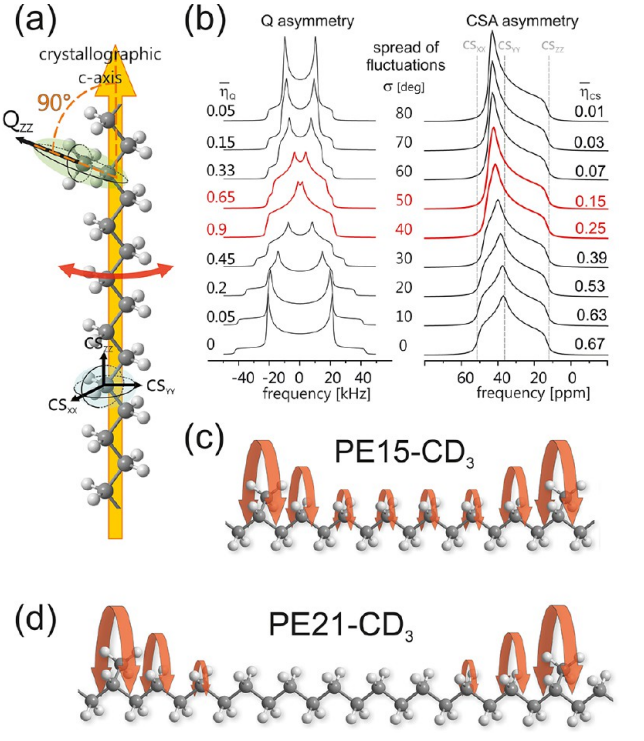

FIGURE 8. Computed ^{2}H and ^{13}C NMR powder line shapes for a Gaussian distributed rotational fluctuation (Figure 3b) around the crystallographic *c*-axis of crystalline PE, according to the motional models presented in panels c and d. Reproduced in part from ref 36. Copyright 2009 Wiley.

Phenylene Motion in Amorphous Polymers. As mentioned in the Introduction, phenyl and phenylene flips are

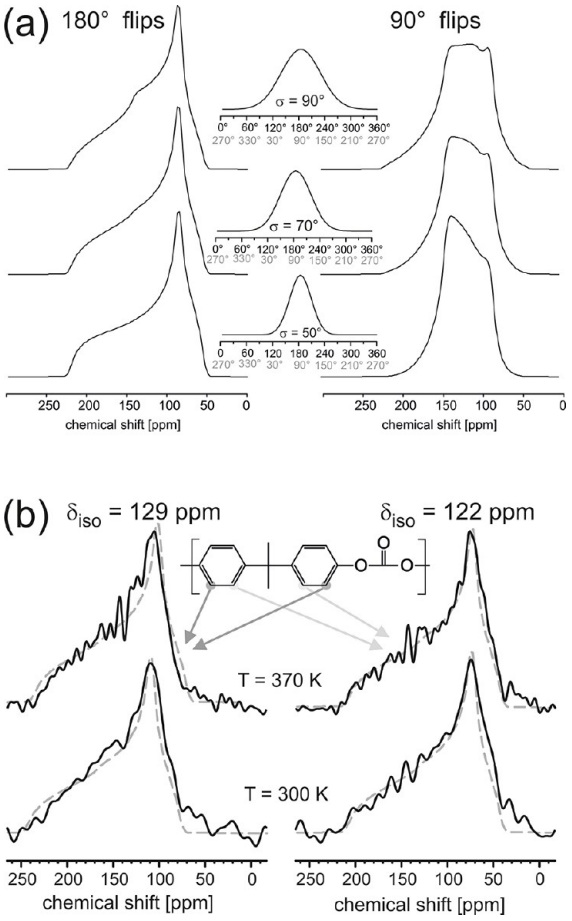

FIGURE 9. Heterogeneous phenylene dynamics in poly(carbonate).[41] (a) Line shape simulations for motionally narrowed ^{13}C NMR spectra with a heterogeneous Gaussian distributions of flip angles centered at 180° and 90° with different standard deviations σ as indicated. (b) Experimental ^{13}C NMR spectra for the two distinct phenylene carbon positions in poly(carbonate) fitted to a heterogeneous Gaussian distribution with full width at half-maximum of 80° of flip angles centered at 180°, dashed line.

ubiquous in synthetic and natural macromolecules and were the first dynamic process clearly identified after the advent of ^2H solid-state NMR. Moreover, they were first observed in bisphenol A polycarbonate (PC), one of the most studied yet still controversial systems as far as sub-T_g dynamics and its relation to ductility is concerned.[37] From ^2H NMR line shapes, large angle phenylene rotations described by 180° flips augmented by additional fluctuations were identified at room temperature and above. Such 180° flips were subsequently confirmed by ^{13}C NMR line shape studies, and their distributions in both time[38] and amplitude were characterized in detail by ^2H NMR.[39] The time scale of the phenylene motion is in remarkable agreement with that of sub-T_g mechanical relaxation. Thus, the phenylene motion seemed well characterized. Recently, the sub-T_g dynamics of PC at ambient temperatures was also studied by quasielastic

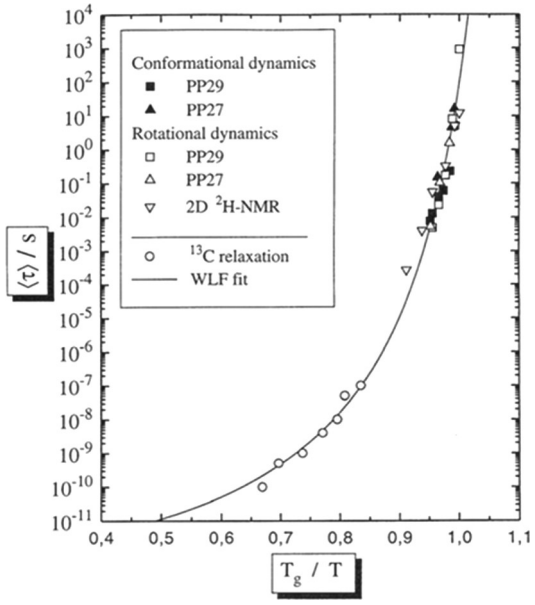

FIGURE 10. Mean correlation times for the chain dynamics of poly(propylene) from different NMR experiments. For details, see ref 43.

neutron scattering,[40] and it was concluded that in addition to 180° flips, the phenylene rings in PC exhibit flips by 90° with correlation times in the range between 1 ns and 1 ps, as the increase of the quasielastic scattering intensity above room temperature could not be accounted for by well-defined 180° flips alone. With advanced 2D NMR techniques probing the ^{13}C CSA, the geometry of the phenylene motion can be probed differently than via ^2H quadrupole coupling, because the unique directions of the two interactions are mutually perpendicular. As can be seen in Figure 9a, 180° and 90° flips result in vastly different line shapes, yet the experimental spectra in Figure 9b show no evidence of the latter. Instead, the phenylene motion in the glassy state displays a heterogeneous distribution of rotational angles, about 80° in width, centered at a flip angle of 180°, essentially constant over a wide temperature range.[41] The presence of flip angles differing significantly from 180° readily explains the increase of quasielastic scattering intensity in the neutron data.

Chain Motion in Polymers due to Conformational Transitions. The most characteristic aspect of chain motion in polymers involves *conformational* transitions. These can be detected by 2D ^{13}C MAS NMR, because different conformers exhibit different chemical shifts.[42] By combinination of various NMR techniques, the segmental motion of polymers at the glass transition can be probed over 14 orders of magnitude as demonstrated in Figure 10 for atactic poly(propylene).[43] The typical non-Arrhenius behavior described by the Williams–Landel–Ferry equation is beautifully displayed.

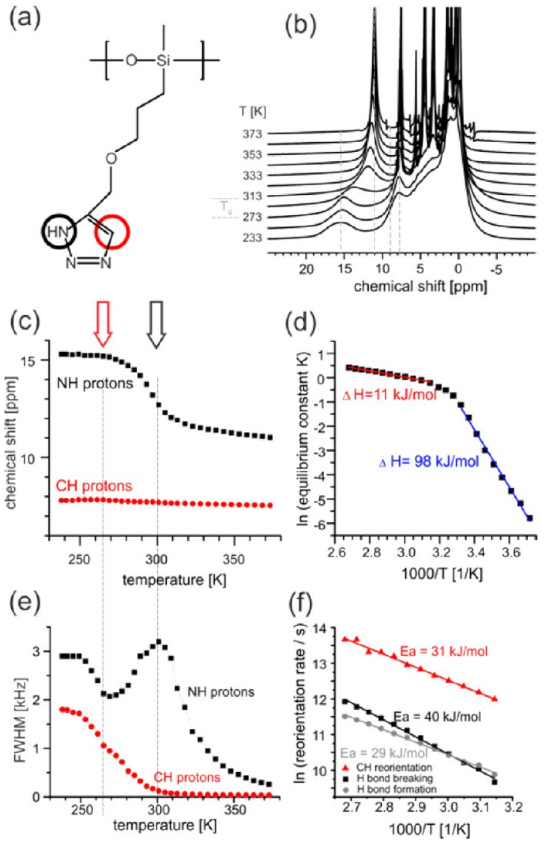

FIGURE 11. (a) Triazole-based proton-conducting polymer. (b) Variable-temperature ^{1}H MAS NMR measurements provide unique details on the dynamic processes involved in the proton conduction process. The thermodynamic behavior (d) can be derived from the chemical shift (c), while rates of different dynamic processes (f) can be followed via the line widths (e). Reproduced in part from ref 46. Copyright 2009 American Chemical Society.

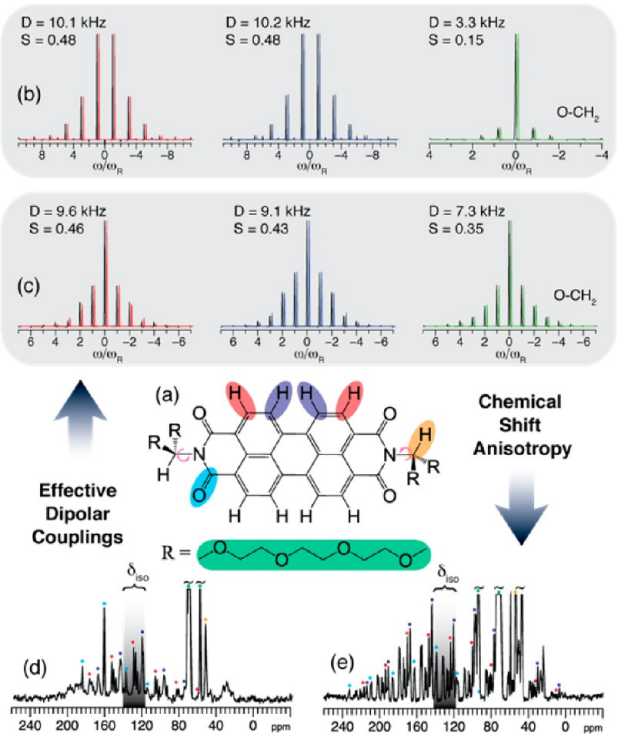

FIGURE 12. (a) Molecular structure of TEG-PDI. Site-specific ^{13}C–^{1}H DDC sideband patterns displaying the dynamical order parameters recorded in the (b) LC and (c) frozen states of TEG-PDI. (d, e) ^{13}C CSA spinning sideband patterns for TEG-PDI in its LC and frozen states, respectively. Reproduced from ref 48. Copyright 2009 Wiley.

At first sight, conformational transitions are expected to involve rotations of individual groups by typical bond angles such as 120°. This can be checked by 2D-exchange NMR, where information about the *geometry* and *time dependence* of the chain dynamics is separated.[2] This showed that the chain dynamics in polymer melts as probed by individual groups involves small angle fluctuations with angular displacements <0.5° followed by "large" angle jumps of 10−25° due to conformational transitions of the chain.[44] Thus, although *bond angles* along the polymer chain undoubtedly change by 120°, the *orientation* of the residues changes much less, because the process is highly cooperative involving many repeat units around the one undergoing the conformational transition. Apparently, the environment in the melt adjusts in such a way that a group involved in a conformational transition is displaced by as little as possible. Thus, fluctuations of building blocks around bond axes are an integral aspect of chain dynamics, yet their amplitudes are considerably smaller in magnitude compared with angular fluctuations in supramolecular aggregates or for molecules trapped in nanopores.[45] It will be interesting to compare these findings for synthetic polymers with conformational transitions in ordered or partially disordered proteins.

Proton-Conducting Materials. Novel and water-free proton-conducting materials for high-temperature applications are based on mobile amphoteric groups covalently attached to a polymer backbone or other supporting materials. Phosphonic acid-based proton conductors, already discussed above, are prominent examples, where NMR methods are able to probe the structure of the local hydrogen-bonding network as well as the proton-conduction mechanism in great detail. Alternative anhydrous proton conductors use aromatic heterocycles such as imidazole or triazole. In these materials, the proton conduction is closely related to the molecular mobility of the aromatic moieties. Simple temperature-dependent ^{1}H MAS NMR spectra, Figure 11b, are able to elucidate the microscopic proton transport in great detail. Changes in the thermodynamic equilibrium of the hydrogen-bonding network alter the isotropic ^{1}H chemical shift of hydrogen-bonding sites, while hydrogen-bonding exchange, as well as molecular reorientation, affects the line width of the NMR signals.

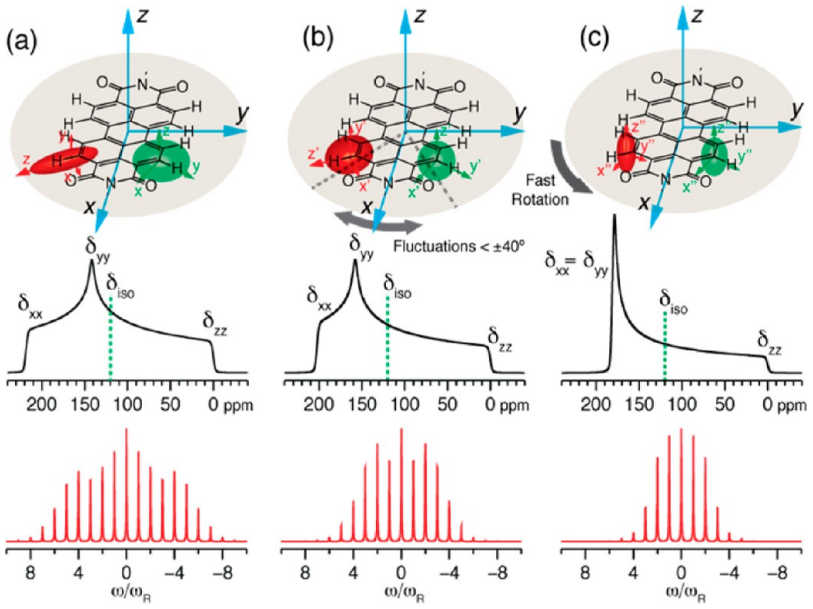

FIGURE 13. Motional averaging of the anisotropic $^{13}C-^{1}H$ DDC and ^{13}C CSA tensors associated with the aromatic core for TEG-PDI under (a) static conditions, (b) fast-limit angular fluctuations, and (c) rapid disk rotation, respectively. Reproduced from ref 48. Copyright 2009 Wiley.

The complete analysis of temperature-dependent ^{1}H MAS NMR spectra has been performed for a triazole-based proton-conducting polymer with a flexible siloxane backbone, Figure 11a.[46] The observed low-temperature process ($T < 300$ K) with substantial enthalpy and entropy changes was assigned to structural changes at the glass transition, while the high-temperature process is related to structural diffusion of protons in the material. The latter shows a low reaction enthalpy, which is favorable for anhydrous proton transport at high operation temperatures. A detailed line width analysis for NH and CH sites of the triazole ring reveals that on average four to five molecular fluctuations of the triazole ring are needed to accomplish proton hopping between different triazole rings.[46] The transition between the high- and the low-temperature regimes is observed at the same temperature in NMR and proton conductivity. Thus, the molecular motion of the triazole ring is crucial for the proton conductivity of the material. However, the activation enthalpy for the hydrogen bond breaking is significantly lower than that of the proton conductivity. This suggests that other thermally activated processes in addition to local breaking and formation of hydrogen bonds are essential for the macroscopic proton conduction.

Molecular Wires based on Discotic Liquid Crystals (DLCs). Nanosized polycyclic aromatic hydrocarbons (PAH) are currently of broad scientific interest due to their potential application as conducting molecular wires. The disk-shaped PAH molecules form π-stacks where charge mobility can occur parallel to the stacking axis. Critical for the charge-carrier properties are disk size, shape, and periphery, allowing control of the self-assembly.[47] We have recently studied two such disk-shaped molecules that form molecular wires in their crystalline (Cr) and liquid crystalline (LC) phases to determine the packing and specific molecular dynamics of the disks.[48,49]

The first is based on perylenetetracarboxdiimide (PDI) end-functionalized with tri(ethylene glycol) (TEG) (Figure 12a). In its LC phase, $S_{D,CH}$ values just below 0.5 were determined (Figure 12b), characteristic of complete disk rotation and small out-of-plane excursions (see Figure 13c). Combined with wide-angle X-ray scattering (WAXS), the rotation was attributed to a cooperative motion of the disks around the columnar axis.[48] In the Cr phase of TEG-PDI $S_{D,CH}$ is similar to the LC phase (Figure 12c). Therefore, we considered in addition the site-specific ^{13}C CSA. As stated above, complete axial rotation renders both tensors axially symmetric, but with very different magnitudes. The $^{13}C-^{1}H$ DDC sideband patterns in Figure 12b, c cannot distinguish between axial rotation and angular fluctuations (see Figure 4), whereas the ^{13}C CSA sideband patterns in Figure 12d,e, as the nonaxial symmetry, can be observed. These show that TEG-PDI in its frozen state performs angular fluctuations with amplitudes up to $\pm 40°$.

Another DLC forming molecular π-stacks is based on a C_3-symmetric hexa-peri-hexabenzocoronene (HBC), Figure 14a. In its Cr phase, $S_{D,CH}$ for the HBC core indicate rigid columns in agreement with WAXS results. Increasing the temperature to the LC phase showed a drastic reduction of $S_{D,CH}$ down to 0.15. This suggests a complex disk motion, resulting from a

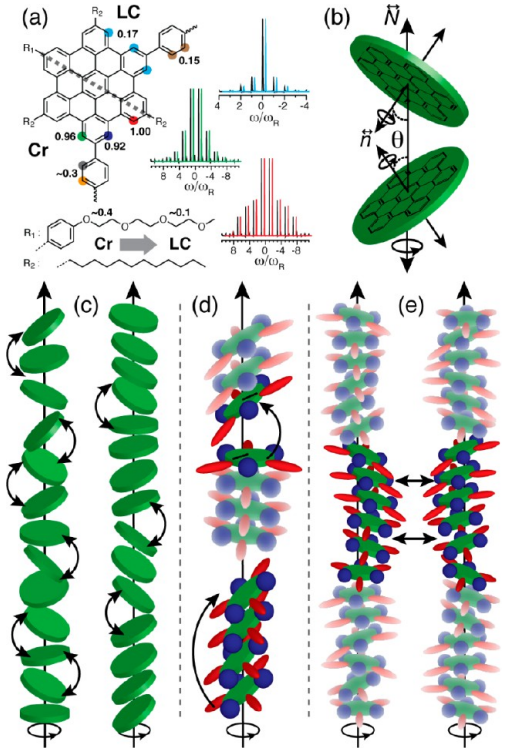

FIGURE 14. (a) Site-specific order parameters for the C_3-symmetric HBC molecule. (b) Double disk rotation around two axes. (c) Homogeneous (left) and heterogeneous (right) disorder along the column axis of a DLC. These can include fast and slow dynamic intracolumnar processes: (d) a single disk jumps from one molecular segment to another, or a whole group of molecules changes their orientation cooperatively, and (e) molecular segments can exchange between columns on the longer time scale. Reproduced from ref 49. Copyright 2011 American Physical Society.

homogeneous or heterogeneous stacking disorder as illustrated in Figure 14c. In the heterogeneous scenario, collective columnar rotation of the disks inclined at an angle $\pm\theta$ to the column axis is expected. From the ^{13}C CSA powder line shape, the inclination angle of the disks was determined as $\theta \approx 43°$.[49] In addition to the collective rotation of the stacks around the column axis, intra- and intercolumnar exchange of disks between molecular segments or even flipping of whole segments from $+\theta$ to $-\theta$ can be envisaged as illustrated in Figure 14d,e. This motion is consistent with the double disk rotation shown in Figure 14b.

Concluding Remarks

This Account provides an introduction to the basics of studying molecular dynamics by solid-state NMR and reviews representative applications to functional macromolecular systems. More complex NMR methods, such as multidimensional techniques[1] and multiple-quantum NMR[50] are, however, needed to cope with the complexity of today's polymer systems. The most severe limitation of NMR is, of course, its low sensitivity. Several promising approaches have emerged and are in the focus of method development today.[51] They are covered in several contributions in this Special Issue. Such developments are particularly important for applications of NMR to studies of functional materials and surfaces. This also encompasses the development of new NMR detectors and detection schemes, which, combined with the advances in NMR sensitivity gains, will pave the way for studies of thin films and other volume-limited samples in their operational environments.

M.R.H. thanks the Carlsberg Foundation for a Postdoctoral Research Fellowship. We are grateful to Dr. Volker Macho for stimulating discussions and his continuing efforts in improving the NMR WEBLAB to suit our scientific problems.

BIOGRAPHICAL INFORMATION

Dr. Michael Ryan Hansen received his Ph.D. from Aarhus University in 2006 for his work on quadrupolar nuclei in heterogeneous catalysis and inorganic materials studied via solid-state NMR and DFT calculations. In 2007, he joined the group of Prof. Hans Wolfgang Spiess at the Max Planck Institute for Polymer Research (MPI-P) as a Carlsberg Foundation Postdoctoral Research Fellow. In 2010, he was appointed research group leader with emphasis on supramolecular systems. His current scientific interests focus on applying solid-state NMR and other methods to understand the complex interplay between structure and dynamics in π-conjugated polymers and oligomers as used in organic electronics.

Dr. Robert Graf graduated at the University of Frankfurt in the field of solid-state physics and switched for his Ph.D. work on double-quantum NMR studies of amorphous polymers under fast magic-angle spinning conditions under the supervision of Prof. Hans Wolfgang Spiess at the MPI-P. In 1998, he became a staff member leading the solid-state NMR group. His main research interests focus the development of NMR methods tailored for studies of local structures and molecular dynamics in partially ordered organic systems and novel functional materials.

Prof. Hans Wolfgang Spiess received his Ph.D. at the University of Frankfurt, Germany, in 1968. He subsequently carried positions as Research Associate at Florida State University (1968–1970), the Max Planck Institute, Heidelberg (1970–1975), and the University of Mainz (1975–1978). He was Professor at the University of Mainz (1978–1980), University of Münster (1981–1982), and University of Bayreuth (1983–1984) before he became Director at the newly founded MPIP-P, Mainz, in 1984, a position he held until his retirement in fall 2012. His scientific interests were solid-state NMR and pulsed EPR and its applications in polymer science and supramolecular functional systems.

FOOTNOTES

*E-mail addresses: mrh@mpip-mainz.mpg.de; graf@mpipmainz.mpg.de; spiess@mpip-mainz.mpg.de.
The authors declare no competing financial interest.

REFERENCES

1 Schmidt-Rohr, K.; Spiess, H. W. *Multidimensional Solid-State NMR and Polymers*; Academic Press: New York, 1994.

2 Spiess, H. W. Structure and dynamics of solid polymers from 2D- and 3D-NMR. *Chem. Rev.* **1991**, *91*, 1321–1338.

3 Brown, S. P.; Spiess, H. W. Advanced solid-state NMR methods for the elucidation of structure and dynamics of molecular, macromolecular, and supramolecular systems. *Chem. Rev.* **2001**, *101*, 4125–4155.

4 deAzevedo, E. R.; Bonagamba, T. J.; Reichert, D. Molecular dynamics in solid polymers. *Prog. Nucl. Magn. Reson. Spectrosc.* **2005**, *47*, 137–164.

5 Demus, D., Goodby, J., Gray, G., Spiess, H. W., Vill, V., Eds. *Fundamentals*; Handbook of Liquid Crystals; Wiley-VCH: Weinheim, Germany, 1998; Vol. 1.

6 Kremer, F.; Schönhals, A. *Broadband Dielectric Spectroscopy*; Springer: Berlin, Germany, 2003.

7 Berne, B. J.; Pecora, R. *Dynamic Light Scattering: With Applications to Chemistry, Biology and Physics*; Wiley: New York, 1976.

8 Strobl, G. R. *The Physics of Polymers: Concepts for Understanding Their Structures and Behavior*; Springer: Heidelberg, 2007.

9 The Gaussian distribution function is defined as $n(\tau_c) \propto e^{-(\ln(\tau_c)-\ln(\tau_{c,0}))^2/(2\sigma^2)}$; $\tau_{c,0} = 100$; $\sigma = \ln(50)$.

10 Vold, R. L.; Hoatson, G. L. Effects of jump dynamics on solid state nuclear magnetic resonance line shapes and spin relaxation times. *J. Magn. Reson.* **2009**, *198*, 57–72.

11 Larsen, F. H. Simulation of Molecular Motion of Quadrupolar Nuclei in Solid-State NMR Spectra. In *Annual Reports on NMR Spectroscopy*; Elsevier: London, 2010; Vol. 71; pp 103−137.

12 Macho, V.; Brombacher, L.; Spiess, H. W. The NMR-WEBLAB: An internet approach to NMR lineshape analysis. *Appl. Magn. Reson.* **2001**, *20*, 405–432.

13 http://weblab.mpip-mainz.mpg.de/weblab/. Note that care should be taken when choosing cone (θ) and jump angles (φ) for comparison with experimental data.

14 Schanda, P.; Huber, M.; Boisbouvier, J.; Meier, B. H.; Ernst, M. Solid-state NMR measurements of asymmetric dipolar couplings provide insight into protein side-chain motion. *Angew. Chem., Int. Ed.* **2011**, 11005–11009.

15 Krushelnitsky, A.; deAzevedo, E.; Linser, R.; Reif, B.; Saalwächter, K.; Reichert, D. Direct observation of millisecond to second motions in proteins by dipolar CODEX NMR spectroscopy. *J. Am. Chem. Soc.* **2009**, *131*, 12097–12099.

16 Cady, S. D.; Schmidt-Rohr, K.; Wang, J.; Soto, C. S.; Degrado, W. F.; Hong, M. Structure of the amantadine binding site of influenza M2 proton channels in lipid bilayers. *Nature* **2010**, *463*, 689–692.

17 Spiess, H. W. Interplay of structure and dynamics in macromolecular and supramolecular systems. *Macromolecules* **2010**, *43*, 5479–5491.

18 Vila, J. A.; Scheraga, H. A. Assessing the accuracy of protein structures by quantum mechanical computations of $^{13}C^{\alpha}$ chemical shifts. *Acc. Chem. Res.* **2009**, *42*, 1545–1553.

19 Harris, R. K.; Wasylishen, R. E.; Duer, M. J. *NMR Crystallography*; Wiley: Chichester, U.K., 2009.

20 Dudenko, D.; Kiersnowski, A.; Shu, J.; Pisula, W.; Sebastiani, D.; Spiess, H. W.; Hansen, M. R. A strategy for revealing the packing in semicrystalline pi-conjugated polymers: Crystal structure of bulk poly-3-hexyl-thiophene (P3HT). *Angew. Chem., Int. Ed.* **2012**, *51*, 11068–11072.

21 Percec, V.; Peterca, M.; Tadjiev, T.; Zeng, X.; Ungar, G.; Leowanawat, P.; Aqad, E.; Imam, M. R.; Rosen, B. M.; Akbey, U.; Graf, R.; Sekharan, S.; Sebastiani, D.; Spiess, H. W.; Heiney, P. A.; Hudson, S. D. Self-assembly of dendronized perylene bisimides into complex helical columns. *J. Am. Chem. Soc.* **2011**, *133*, 12197–12219.

22 Elmahdy, M. M.; Floudas, G.; Mondeshki, M.; Spiess, H. W.; Dou, X.; Müllen, K. Origin of the complex molecular dynamics in functionalized discotic liquid crystals. *Phys. Rev. Lett.* **2008**, *100*, No. 107801.

23 Yao, Y. F.; Graf, R.; Spiess, H. W.; Rastogi, S. Restricted segmental mobility can facilitate medium-range chain diffusion: A NMR study of morphological influence on chain dynamics of polyethylene. *Macromolecules* **2008**, *41*, 2514–2519.

24 Fritzsche, M.; Bohle, A.; Dudenko, D.; Baumeister, U.; Sebastiani, D.; Spiess, H. W.; Hansen, M. R.; Höger, S. Empty helical nanochannels with adjustable order from low-symmetry macrocycles. *Angew. Chem., Int. Ed.* **2011**, *50*, 3030–3033.

25 He, Y.; Lutz, T. R.; Ediger, M. D.; Ayyagari, C.; Bedrov, D.; Smith, G. D. NMR experiments and molecular dynamics simulations of the segmental dynamics of polystyrene. *Macromolecules* **2004**, *37*, 5032–5039.

26 Spiess, H. W. In *NMR Basic Principles and Progress*; Diehl, P., Fluck, E., Kosfeld, R., Eds.; Springer: Berlin, 1978; Vol. 15, pp 55−214.

27 Schmidt, J.; Hutter, J.; Spiess, H. W.; Sebastiani, D. Beyond isotropic tumbling models: Nuclear spin relaxation in liquids from first principles. *ChemPhysChem* **2008**, *9*, 2313–2316.

28 Floudas, G.; Spiess, H. W. Self-assembly and dynamics of polypeptides. *Macromol. Rapid Commun.* **2009**, *30*, 278–298.

29 Lee, Y. J.; Murakhtina, T.; Sebastiani, D.; Spiess, H. W. H-2 solid-state NMR of mobile protons: It is not always the simple way. *J. Am. Chem. Soc.* **2007**, *129*, 12406–12407.

30 Graf, R. New proton conducting materials for technical applications: What can we learn from solid state NMR studies? *Solid State Nucl. Magn. Reson.* **2011**, *40*, 127–133.

31 Grey, C. P.; Dupre, N. NMR studies of cathode materials for lithium-ion rechargeable batteries. *Chem. Rev.* **2004**, *104*, 4493–4512.

32 Lee, Y. J.; Bingoel, B.; Murakhtina, T.; Sebastiani, D.; Meyer, W. H.; Wegner, G.; Spiess, H. W. High-resolution solid-state NMR studies of poly(vinyl phosphonic acid) proton-conducting polymer: Molecular structure and proton dynamics. *J. Phys. Chem. B* **2007**, *111*, 9711–9721.

33 Hinderberger, D.: EPR Spectroscopy in Polymer Science. In *EPR Spectroscopy Applications in Chemistry and Biology*; Springer: Berlin, Heidelberg, 2011; Vol. 321, pp 67−89.

34 Jeschke, G. DEER distance measurements on proteins. *Annu. Rev. Phys. Chem.* **2012**, *63*, 419–446.

35 Yao, Y.-F.; Graf, R.; Spiess, H. W.; Lippits, D. R.; Rastogi, S. Morphological differences in semicrystalline polymers: Implications for local dynamics and chain diffusion. *Phys. Rev. E* **2007**, *76*, No. 060801.

36 Wei, Y.; Graf, R.; Sworen, J. C.; Cheng, C.-Y.; Bowers, C. R.; Wagener, K. B.; Spiess, H. W. Local and collective motions in precise polyolefins with alkyl branches: A combination of H-2 and C-13 solid-state NMR spectroscopy. *Angew. Chem., Int. Ed.* **2009**, *48*, 4617–4620.

37 Monnerie, L.; Lauprêtre, F.; Halary, J. L. Investigation of solid-state transitions in linear and cross-linked amorphous polymers. *Adv. Polym. Sci.* **2005**, *187*, 35–213.

38 Wehrle, M.; Hellmann, G. P.; Spiess, H. W. Phenylene motion in polycarbonate and polycarbonate/additive mixtures. *Colloid Polym. Sci.* **1987**, *265*, 815–822.

39 Hansen, M. T.; Boeffel, C.; Spiess, H. W. Phenylene motion in polycarbonate: Influence of tensile stress and chemical modification. *Colloid Polym. Sci.* **1993**, *271*, 446–453.

40 Arrese-Igor, S.; Arbe, A.; Alegrgria, A.; Colmenero, J.; Frick, B. Sub-Tg dynamics in polycarbonate by neutron scattering and its relation with secondary g-relaxation. *J. Chem. Phys.* **2005**, *123*, No. 014907.

41 Graf, R.; Ewen, B.; Spiess, H. W. Geometry of phenylene motion in polycarbonate from NMR spectroscopy and neutron scattering. *J. Chem. Phys.* **2007**, *126*, No. 041104.

42 Tonelli, A. E.; Schilling, F. C. Carbon-13 NMR chemical shifts and the microstructure of polymers. *Acc. Chem. Res.* **1981**, *14*, 233–238.

43 Zemke, K.; Schmidt-Rohr, K.; Spiess, H. W. Polymer conformational structure and dynamics at the glass transition studied by multidimensional 13C NMR. *Acta Polym.* **1994**, *45*, 148–159.

44 Tracht, U.; Heuer, A.; Spiess, H. W. Geometry of reorientational dynamics in supercooled poly(vinyl acetate) studied by 13C two-dimensional nuclear magnetic resonance echo experiments. *J. Chem. Phys.* **1999**, *111*, 3720.

45 Albunia, A. R.; Graf, R.; Grassi, A.; Guerra, G.; Spiess, H. W. Geometry of complex molecular motions of guest molecules in polymers from solid state ^{2}H NMR. *Macromolecules* **2009**, *42*, 4929–4931.

46 Akbey, Ü.; Granados-Focil, S.; Coughlin, E. B.; Graf, R.; Spiess, H. W. ^{1}H solid-state NMR investigation of structure and dynamics of anhydrous proton conducting triazole-functionalized siloxane polymers. *J. Phys. Chem. B* **2009**, *113*, 9151–9160.

47 Feng, X.; Marcon, V.; Pisula, W.; Hansen, M. R.; Kirkpatrick, J.; Grozema, F.; Andrienko, D.; Kremer, K.; Müllen, K. Towards high charge-carrier mobilities by rational design of the shape and periphery of discotics. *Nat. Mater.* **2009**, *8*, 421–426.

48 Hansen, M. R.; Schnitzler, T.; Pisula, W.; Graf, R.; Müllen, K.; Spiess, H. W. Cooperative molecular motion within a self-assembled liquid-crystalline molecular wire: The case of a TEG-substituted perylenediimide disc. *Angew. Chem., Int. Ed.* **2009**, *48*, 4621–4624.

49 Hansen, M. R.; Feng, X.; Macho, V.; Müllen, K.; Spiess, H. W.; Floudas, G. Fast and slow dynamics in a discotic liquid crystal with regions of columnar order and disorder. *Phys. Rev. Lett.* **2011**, *107*, No. 257801.

50 Spiess, H. W.: Double-quantum NMR spectroscopy of dipolar-coupled spins under fast magic-angle spinning. In *Encyclopedia of Magnetic Resonance*; John Wiley & Sons, Ltd: Chichester, U.K., 2012.

51 Spiess, H. W. NMR spectroscopy: Pushing the limits of sensitivity. *Angew. Chem., Int. Ed.* **2008**, *47*, 639–642.